Cite this article
Azhari A, Isfahani HS and Heydari KE
Effect of geometry and material of municipal solid waste landfills on seismic response.
Proceedings of the Institution of Civil Engineers – Waste and Resource Management,
https://doi.org/10.1680/jwarm.20.00040

Research Article
Paper 2000040
Received 01/06/2021;
Accepted 01/06/2021

Keywords: landfills/mathematical modelling/seismic engineering

Waste and Resource Management

ICE Publishing

Effect of geometry and material of municipal solid waste landfills on seismic response

Amin Azhari
Assistant Professor, Department of Mining Engineering, Isfahan University of Technology, Isfahan, Iran (corresponding author: aazhari@iut.ac.ir)

Hajar Share Isfahani
Assistant Professor, Department of Civil Engineering, Isfahan University of Technology, Isfahan, Iran

Keyvan Ebneali Heydari
MSc student, Department of Mining Engineering, Isfahan University of Technology, Isfahan, Iran

The stability of municipal solid waste (MSW) landfills is a significant environmental concern. The performance of landfills during earthquakes should be evaluated to ensure their stability. The geometry and material types of MSW landfills are the main factors affecting their seismic response. In this study, the individual and coupled impact of these factors is investigated using numerical analyses. Amplification factors ($AFs = Acc_{surface}/Acc_{base}$) are investigated for six common MSW landfill types, namely canyon type, hill type, side-hill types 1 and 2 and stepped-base types 1 and 2. The results show that landfill types have significantly different behaviours due to their geometry and waste material properties. For low stiffness contrasts, the stepped-base landfill type has the minimum and the hill type experiences the maximum AF, 1.74 and 3.53, respectively. However, for high stiffness contrasts, the canyon type has the minimum AF (0.46) due to the effect of damping and thickness of the waste. Therefore, the proper geometry of the MSW landfills should be designed for specific waste material properties according to the seismic response.

Notation

$\mathbf{C}$	damping matrix
$\mathbf{M}$	mass matrix
$\mathbf{K}$	stiffness matrix
c	cohesion
C_s	shear wave velocity
E	elastic modulus
f_{max}	maximum frequency of the waves carrying energy
G	elastic shear modulus
α	mass-proportional damping constant
β	stiffness-proportional damping constant
γ	unit weight
ξ	damping ratio
φ	friction angle
ϑ	Poisson's ratio
ω	natural frequency

1. Introduction

Environmental pollution from waste materials is one of the significant hazard concerns for human lives (Hossain *et al*., 2011; Isfahani *et al*., 2019; Misra and Pandey, 2005). More than 2.1 billion tonnes of municipal solid waste (MSW), one of the main significant types of waste materials, are produced annually around the world (IBRD, 2019). MSW is usually disposed in geo-structures named landfills, which have their environmental concerns, including soil, air and water contamination, that have to be considered in sustainable development decision making (Feng *et al*., 2018; Shu *et al*., 2018). Various types of failures from liner cracks to minor slope failures have occurred on landfills subjected to strong earthquakes during the construction of liner systems and waste filling, or after closure of the landfill. For instance, 22 landfills in California, USA were subjected to the Northridge earthquake of 17 January 1994 with a magnitude of 6.7; one suffered significant damage, four experienced moderate damage and 17 had minor or no damage. Most of the damage caused cracking in the liner and the cover soil or tears in the geomembrane. Investigation on the performance of ten landfills, also in California, USA, during the Loma Prieta earthquake of 17 October 1989 with a magnitude of 7.1 shows major and minor crack displacements of the liners typically between 25 and 75 mm and one with a minor downslope cover soil movement. Studies show that the recorded peak ground acceleration (PGA) has a direct relation with the intensity of the damages. For example, during the Northridge event, the Chiquita Canyon landfill, subjected to a high free-field PGA of 0.39***g***, suffered the most notable damage, compared with landfills subjected to PGAs of lower than 0.2***g***; the damage consisted of tears between 3 and 23 m in length within the geomembrane liner. Bradley and Lopez Canyon landfills were subjected to an estimated free-field PGA of 0.45***g*** and 0.44***g***, respectively, causing a local tear in the geotextile overlying the side-slope liner. In this regard, evaluation of the performance of landfills during an earthquake becomes a significant issue for geotechnical engineers designing MSW landfills.

The seismic response to these structures is mainly caused by two groups of characteristics: source and site effects. Source effects are defined by the source of the earthquake, such as earthquake magnitude, frequency, epicentral distance, depth and duration, which are mostly uncontrollable by engineers (Azhari and Ozbay, 2016, 2018; Havenith *et al.*, 2003; Meunier *et al.*, 2008). However, site characteristics, including landfill geometry and material stiffness contrast, are mainly controlled by engineering design. Various research studies have evaluated the impact of site effects on earthquake response of slopes (Azhari and Ozbay, 2018; Bourdeau and Havenith, 2008; Del Gaudio and Wasowski, 2011; Havenith *et al.*, 2002, 2003; Ling *et al.*, 2015; Meunier *et al.*, 2008; Moore *et al.*, 2011; Sepúlveda *et al.*, 2005; Seyhan and Stewart, 2014; Si and Midorikawa, 2000; Wang and Hao, 2002).

Azhari and Ozbay (2018) examined the effect of epicentral distance and depth on the earthquake-triggered failures of natural slopes and tailings dams. The results showed that an epicentral distance and depth of less than 100 and 40 km, respectively, may cause failures on these types of slopes. Azhari and Ozbay (2017) have numerically investigated the effect of valley and hill topographies, as well as the soft topsoil layer, on the wave acceleration amplification of the slopes. The analyses showed that in hill geometries with soft topsoil layers, the wave may amplify up to 16 times compared with valley geometries. Havenith *et al.* (2003) evaluated the seismic amplification of the Tien Shan Range, China, according to the morphology and topography of the region. The study also numerically examined the surface layer- and topography-dependent amplifications using two- and three-dimensional modelling. Meunier *et al.* (2008) investigated the earthquake-triggered failures near Northridge, California, Chi-Chi, Taiwan and the Finisterre Mountains of Papua New Guinea. It was observed that most failures occurred on ridge crests and diverse geological substrate locations. Moore *et al.* (2011) evaluated the dynamic response of a large unstable rock slope at Randa, Switzerland. The discrete-element numerical approach was used and showed that the highly fractured top section of the slope is mostly prone to failures and that site effects contributed less to the seismic behaviour of hard rock slopes. Sepúlveda *et al.* (2005) conducted a study on the Pacoima Canyon, California, which was exposed to the 1994 Northridge earthquake ($M_w = 6.7$). The results depicted a PGA of 1.6$\boldsymbol{g}$ recorded at ridges and less than 0.5$\boldsymbol{g}$ at the bottom of the canyon, verifying the occurrence of topographic amplification. Si and Midorikawa (2000) studied the recorded ground motions from 21 earthquakes in Japan. The data included 856 records for PGA and 394 records for peak ground velocity. The data were analysed based on the epicentral distance and focal depth where their correlations with site effects were examined. The results show that generally deeper focal depth causes stronger ground motion. Wang and Hao (2002) conducted a numerical parametric study evaluating the effect of material variation on the slope's seismic response. It was found that the obtained surface motions vary substantially if the random variants of soil properties and their saturation levels are considered in the analysis.

Previous studies show a significant seismic response amplification due to the stiffness contrast between the bedrock and the topsoil layer and sharp topographies such as ridges and convex geometries. Amplification factor ($AF = PGA_{surface}/PGA_{earthquake}$) as the defining parameter for seismic responses of the structures was commonly utilised in these studies; it was defined in the range 2–16, based on the slope geomechanical and topographical characteristics. Although many research studies have been performed on the seismic stability of natural slopes, few studies have been conducted on the seismic response of landfills, most of which used traditional pseudo-static, pseudo-dynamic and Newmark methods (Bray *et al.*, 1995; Bray and Rathje, 1998; Chen *et al.*, 2008; Choudhury and Savoikar, 2011a, 2011b; Kramer and Smith, 1997; Ling and Leshchinsky, 1997; Rathje and Bray, 2001).

Bray *et al.* (1995) conducted pseudo-static stability analyses of the seismically induced deformation of landfills. The results showed that the maximum horizontal acceleration for the waste material would be twice that for the bedrock. Bray and Rathje (1998), in another study, used the Newmark approach to estimate the displacements caused by various earthquakes on typical MSW landfills with heights of 10–90 m. Ultimately, charts have been developed to predict the seismic-induced displacements of these landfill structures. Chen *et al.* (2008) evaluated the permanent seismic displacement of landfills along the liners under various site conditions using the Newmark method. The Newmark analyses showed that the frequency and amplitude of the bedrock motion would vary the permanent displacements of the landfill liners. Choudhury and Savoikar (2011a, 2011b) performed two studies in 2011, using pseudo-static and pseudo-dynamic analyses on the stability of landfills under seismic loading. It was concluded that the pseudo-static analysis has limitations considering the variation of seismic inertial forces with time. Additionally, they investigated the effects of the vertical components of the shear and primary waves, which may have a serious effect on the seismic response of these structures. As a result, they implemented the pseudo-dynamic approach in their next study to overcome these limitations. Kramer and Smith (1997) developed a modified Newmark approach. Unlike the conventional Newmark method, which neglects the dynamic response of the material above the failure surface, this modified approach considers the effects of permanent displacements of the material above the failure surface. Rathje and Bray (2001) investigated the material depth of the upper sliding layer using numerical finite-element and Newmark methods. It was shown that the Newmark approach will give a conservative result for deep overlaying material while more caution should be warranted for the shallow layers, compared with the results of numerical analyses.

As noted, there are well-known limitations related to these approaches, such as disregarding the frequency and duration of the seismic wave, as well as the deformation parameters of the ground, considering the failure on an explicit discontinuity, and ignoring the upslope movement of the failure zone on top of the discontinuity. Therefore, none of the conventional approaches considers the actual ground and wave conditions, such as complex geometries and material stiffness contrasts. In contrast, the numerical approach is capable of overcoming these limitations and accommodates wave propagation through various geometries and material properties. However, a limited number of studies have been carried out on the stability and seismic response of landfills using numerical methods. Choudhury and Savoikar (2009) evaluated the seismic response of hill-type landfills based on the foundation characteristics. The numerical analyses showed that the sequence of soft and stiff foundation materials would increase the acceleration AF up to four times. Zania *et al*. (2008) investigated the seismic performance of two landfill geometry types, namely hill and side-hill landfills. It was concluded that the AF is related to the crest width of the hill type and the crest itself shows the highest AF among the monitored points. The hill type generally showed a higher AF due to its convex geometry. According to the literature, there is much to be understood on the seismic response of different landfill geometries with various material properties.

This study aims to evaluate the seismic response of typical landfill geometries and material properties. In this regard, six well-known landfill geometries, along with four levels of material stiffness contrasts, are considered. The AF on the monitored locations for each landfill type with different material characteristics was obtained numerically and compared with previous studies.

2. Numerical assessment of the seismic response

As previously mentioned, the numerical approach could be the most suitable method for the simulation of the seismic response of landfills with various geometries and material characteristics. Among the numerical methods, the Universal Distinct Element Code (UDEC) is the code with the capability of modelling both continuum and discontinuum media. This computer code is able to provide the AF, simulating the geometry and material properties of site effects that would affect the seismic response of

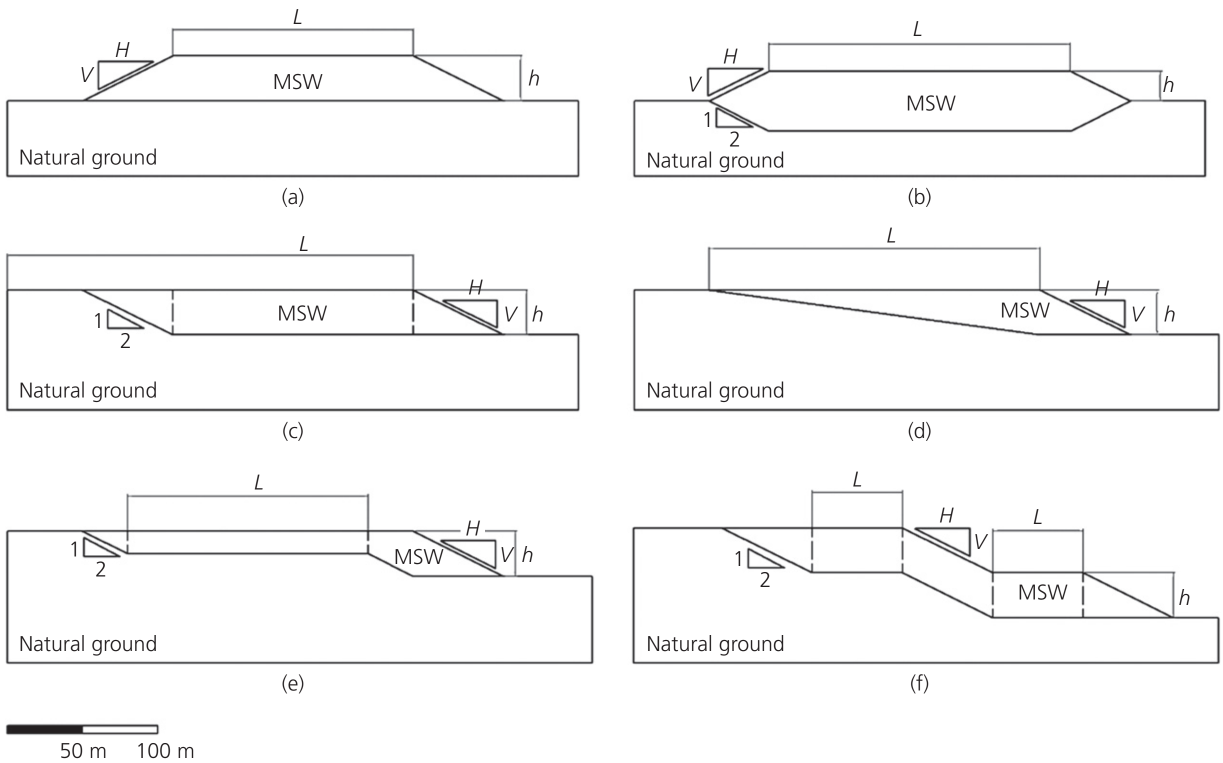

Figure 1. Typical MSW landfill geometries used in the numerical analysis: (a) hill type, (b) canyon type, (c) side-hill type 1, (d) side-hill type 2, (e) stepped-base type, (f) stepped-base and fill type

Table 1. Shear strength parameters for MSW landfills

c: kPa	*φ*: °	Comments	References
23	24	Large direct-shear test on fresh shredded MSW (Edmonton)	Landva and Clark (1990)
19	39	Large direct-shear test on typical fresh MSW (Blackfoot)	Landva and Clark (1990)
16	33	Large direct-shear test on typical fresh MSW (Blackfoot)	Landva and Clark (1990)
0	27	Large direct-shear test on 8-year-old artificial refuse (UNB)	Landva and Clark (1990)
0	41	Large direct-shear test on 8-year-old artificial refuse (UNB)	Landva and Clark (1990)
0	36	Large direct-shear test on typical old MSW (Hantsport)	Landva and Clark (1990)
19	39	Large direct-shear tests on samples from old fill in Calgary	Landva and Knowles (1990)
23	24	Large direct-shear tests on samples from freshly shredded fill in Edmonton	Landva and Knowles (1990)
0	39–53	Direct-shear test at a landfill in southern California	Siegel *et al*. (1990)
25	10	Strength properties of Hong Kong refuse	Cowland *et al*. (1993)
15.7	21	NA	Del Greco and Oggeri (1994)
22	22	NA	Del Greco and Oggeri (1994)
10	23	NA	Fassett *et al*. (1994)
5	34	NA	Houston *et al*. (1995)
10	30	Typical MSW with sample size 150 cm × 150 cm	Houston *et al*. (1995)
2–3	15–20	Triaxial test on 1–3-year-old MSW	Grisolia *et al*. (1995)
24	0	For normal stress less than 30 kPa	Kavazanjian *et al*. (1995)
0	30	For normal stress more than 30 kPa	Kavazanjian *et al*. (1995)
21	17.8	Large direct-shear test on typical fresh MSW (Blackfoot)	Pelkey *et al*. (2001)
5	21.8	Large direct-shear test on shredded MSW (Edmonton)	Pelkey *et al*. (2001)
0	23	Large direct-shear test on wood waste (Edmonton)	Pelkey *et al*. (2001)
12	37	Large direct-shear test on typical MSW (Hantsport NS)	Pelkey *et al*. (2001)
0	26–29	Large direct-shear test on MSW	Pelkey *et al*. (2001)
23.3	9.9	Triaxial test on 1.7-year-old MSW	Zhan *et al*. (2008)
0	39	Triaxial test on 11-year-old MSW	Zhan *et al*. (2008)
10	20	Data from back analysis of MSW	Koelsch *et al*. (2005)
18	22	Suggested friction angle and cohesion data for MSW	Koelsch *et al*. (2005)
15	15	Suggested friction angle and cohesion data for MSW	Koelsch *et al*. (2005)
4–7	10–14	Triaxial test on 5-year-old MSW at 5% strain	Feng (2005)
15–28	14–17	Triaxial test on 5–year-old MSW at 10% Strain	Feng (2005)
30–58	17–19	Triaxial test on 5-year-old MSW at 15% Strain	Feng (2005)
19	28	Data from back analysis of MSW	Merry *et al*. (2005)
9–14	20–29	Direct-shear test and triaxial test	Harris *et al*. (2005)
14	36	Direct-shear test data on fresh MSW with sample size 30 cm × 45 cm	Singh *et al*. (2009b)
10	25.4	Results from a statistical analysis	Jahanfar (2014)
1–40	28–35	Direct-shear test on MSW	Reddy *et al*. (2011)
15	35	NA	Giri and Reddy (2015)
4.7	31.9	Guangming, Shenzhen, China landfill of	Ouyang *et al*. (2017)
10	25–30	New waste	Tano *et al*. (2017)
5	22–24	Old waste	Tano *et al*. (2017)
29	15.7	Direct-shear test on a sample from 4 m depth	Feng *et al*. (2017)
24	19.6	Direct-shear test on a sample from 11 m depth	Feng *et al*. (2017)
18	21.9	Direct-shear test on a sample from 16 m depth	Feng *et al*. (2017)
20	35	NA	Hubert *et al*. (2016)
13.7	22	Direct-shear test on the more degraded wastes	Abreu and Vilar (2017)
4.4	40	Direct-shear test on the less degraded wastes	Abreu and Vilar (2017)
14.5	22.5	Direct-shear test at 25 mm displacement from Ghazipur at Delhi, India	Ramaiah *et al*. (2017)
16.6	33.4	Direct-shear test at 50 mm displacement from Ghazipur at Delhi, India	Ramaiah *et al*. (2017)
6.2	26	Direct-shear test at 25 mm displacement from Ghazipur at Delhi, India	Ramaiah *et al*. (2017)
14.4	34.6	Direct-shear test at 50 mm displacement from Ghazipur at Delhi, India	Ramaiah *et al*. (2017)
10	23	Direct-shear test at 25 mm displacement from Ghazipur at Delhi, India	Ramaiah *et al*. (2017)
11.1	35.4	Direct-shear test at 50 mm displacement from Ghazipur at Delhi, India	Ramaiah *et al*. (2017)
27.5	27.1	Direct-shear test at 25 mm displacement from Ghazipur at Delhi, India	Ramaiah *et al*. (2017)
28.8	40.4	Direct-shear test at 50 mm displacement from Ghazipur at Delhi, India	Ramaiah *et al*. (2017)
20.7	25.8	Direct-shear test at 25 mm displacement from Okhla at Delhi, India	Ramaiah *et al*. (2017)
22.7	38.5	Direct-shear test at 50 mm displacement from Okhla at Delhi, India	Ramaiah *et al*. (2017)
9.9	25.1	Direct-shear test at 25 mm displacement from Okhla at Delhi, India	Ramaiah *et al*. (2017)
16.2	37.4	Direct-shear test at 50 mm displacement from Okhla at Delhi, India	Ramaiah *et al*. (2017)
18.5	21.5	Direct-shear test at 25 mm displacement from Okhla at Delhi, India	Ramaiah *et al*. (2017)
21.3	37.4	Direct-shear test at 50 mm displacement from Okhla at Delhi, India	Ramaiah *et al*. (2017)

NA, not applicable

Table 2. Unit weight data for MSW landfills

γ: kN/m^3	Comments	References
10–14	Dry density	Landva and Knowles (1990)
5–7	Dry density	Del Greco and Oggeri (1994)
3–9	For low compaction waste	Fassett *et al.* (1994)
5–7.8	For medium compaction waste	Fassett *et al.* (1994)
8.8–10.5	For good compaction waste	Fassett *et al.* (1994)
10–12	Dry density	Gabr and Valero (1995)
10.8–12.8	Dry density	Withiam *et al.* (1995)
3.3	Surface	Kavazanjian *et al.* (1995)
12.8	60 m depth	Kavazanjian *et al.* (1995)
16	Average unit weight from the in situ test on Operating Industries, Inc. (OII) landfill Superfund site	Matasović and Kavazanjian (1998)
10–16	Bulk density	Pelkey *et al.* (2001)
10	Bulk density	Machado *et al.* (2002)
9.1	Un-degraded MSW from Dona Juana sanitary landfill	Caicedo *et al.* (2002)
5.3	Poor compaction	Dixon and Jones (2005)
7	Moderate compaction	Dixon and Jones (2005)
9.6	Good compaction	Dixon and Jones (2005)
12.23	NA	Jones and Dixon (2005)
11	NA	Koelsch *et al.* (2005)
10	NA	Dixon *et al.* (2006)
10.4	MSW landfill near Cincinnati, OH, USA	Chugh *et al.* (2007)
9.4	4–6 m depth (a landfill in France)	Stoltz *et al.* (2009)
11.5	6–12 depth (a landfill in France)	Stoltz *et al.* (2009)
11.8	12–17 depth (a landfill in France)	Stoltz *et al.* (2009)
16.6	17–22 depth (a landfill in France)	Stoltz *et al.* (2009)
13.9	22–27 depth (a landfill in France)	Stoltz *et al.* (2009)
16	27–32 depth (a landfill in France)	Stoltz *et al.* (2009)
14.8	32–36 depth (a landfill in France)	Stoltz *et al.* (2009)
10.2	NA	Modak (2010)
11.2–16.2	NA	Reddy *et al.* (2011)
7.8	Obtained from laboratory experiments on US MSW samples	Bareither *et al.* (2010)
15	Borehole density test	Matasovic *et al.* (2011)
14.6	Averages of reported data	Giri and Reddy (2014)
11	Suzhou landfill, China	Zhan *et al.* (2008)
11.1	Statistical analysis from the literature review	Jahanfar (2014)
9.9	NA	Sia and Dixon (2012)
9–12.6	New waste	Tano *et al.* (2016)
10–12.8	Old waste	Tano *et al.* (2016)
10	NA	Hubert *et al.* (2016)
7.2–12.5	From surface to 16 m depth	Hubert *et al.* (2016)
8.1–11	For shallow waste	Abreu and Vilar (2017)
13.8–15.2	For deep waste	Abreu and Vilar (2017)

NA, not applicable

landfills. The geometrical and geomechanical data applied in this numerical modelling are mainly obtained from the published data on most typical MSW landfill types worldwide.

2.1 Considered geometries

As for geometries, there are six major landfill types illustrated in Figure 1, namely, hill type, canyon type, side-hill type 1, side-hill type 2, stepped-base type and stepped-base and fill type. In 2010, Savoikar and Choudhury (2010) proposed these six typical geometries to address the seismic stability for different landfill configurations.

2.2 Material characteristics

A comprehensive study is conducted on the properties of MSW landfills derived from more than 50 studies since 1990. The material properties for the models, considering Mohr–Coulomb as the behaviour model, are derived from the statistical analysis of these data. This analysis is conducted on the shear strength parameters cohesion (c), friction angle (φ), unit weight (γ), Poisson's ratio (ϑ) and elastic modulus (E) of the waste material. Table 1 presents the cohesion and friction angle according to the literature defining the shear strength of the waste based on the Mohr–Coulomb criteria, obtained from either a direct shear or a

Table 3. Various published values for elastic parameters of MSW

E: MPa	ϑ	Comments	References
40–120	NA	Dynamic module from in situ testing	Houston *et al.* (1995)
NA	0.25–0.33	Field measurements of Poisson's ratio from Operating Industries, Inc. (OII) landfill Superfund site	Matasović and Kavazanjian (1998)
5–7	0.25	Landfill in Kahrizak, Tehran, Iran	Fakharian and Taherzadeh (2004)
130	0.3	Data from the landfill of Cincinnati, Ohio, USA	Chugh *et al.* (2007)
0.5	0.3	NA	Jones and Dixon (2005)
NA	0.2–0.3	Large-scale cyclic triaxial testing	Zekkos *et al.* (2008)
0.5–0.7	0.05–0.15	Degradable and compressible (food, yard and animal waste) landfill of Ontario, Canada	Singh *et al.* (2009a)
1.5–3	0.28–0.32	Reinforcing and tensile elements (paper, cardboard, flexible and rigid plastics and tyres) landfill of Ontario, Canada	Singh *et al.* (2009a)
10–20	0.25–0.33	Soil-like material (demolition waste, cover soil and ash) landfill of Ontario, Canada	Singh *et al.* (2009a)
75–110	0.26–0.49	Rigid and incompressible (metals, glass, wood and ceramic) landfill of Ontario, Canada	Singh *et al.* (2009a)
0.7	0.45	During the construction of Coll Cardús landfill	Yu and Batlle (2011)
7	0.3	After construction of Coll Cardús landfill	Yu and Batlle (2011)
0.5	NA	Long term of Coll Cardús landfill	Yu and Batlle (2011)
NA	0.25	The first phase of degradation	Varga (2011)
NA	0.45	The fifth phase of degradation	Varga (2011)
6.1–12.1	NA	Fly ash + 0% quicklime	Fatahi and Khabbaz (2013)
7.7–15.7	NA	Fly ash + 6.7% quicklime	Fatahi and Khabbaz (2013)
10.7–21.5	NA	Fly ash + 13.3% quicklime	Fatahi and Khabbaz (2013)
15.5–27	NA	Fly ash + 20% quicklime	Fatahi and Khabbaz (2013)
19.6–36.1	NA	Fly ash + 26.7% quicklime	Fatahi and Khabbaz (2013)
0.5	0.3	NA	Zamara *et al.* (2014)
1.43	0.1	Intermediate MSW	Sia and Dixon (2012)
2.55	0.1	Stiff MSW	Sia and Dixon (2012)
0.5–1	0.2–0.3	New waste	Tano *et al.* (2017)
1–1.2	0.3–0.4	Old waste	Tano *et al.* (2017)

NA, not applicable

triaxial compressive test. Table 2 shows the commonly available unit weight of the waste material according to its depth, age and compaction condition. The Young's elastic modulus and Poisson's ratio are shown in Table 3, representing the deformability properties of the waste material. Statistical analyses are then conducted on the data obtained for each material characteristic. According to the analyses, the 'best fit' approach is applied to the data and the probability density function (PDF) of each parameter is derived accordingly. Figure 2 shows the statistical PDF along with the mean and standard deviation values for the shear strength, unit weight and elastic deformability parameters of the waste material. From these graphs, the mean value of each parameter is chosen for the analyses. It should be noted that, although the unit weight of the waste material gradually increases with depth, the more frequent value from the data analyses (Figure 2) is considered for the waste material. It should be noted that the mechanical characteristics of the MSW landfill material may change from country to country and city to city. Therefore, a comprehensive literature review is performed to find the most frequent properties. Moreover, the material characteristics, including density, elastic modulus, Poisson's ratio, friction angle and cohesion, may vary with time. However, earlier studies show that elastic modulus is the most controlling factor affecting the seismic response of slopes. Therefore, in this study, a variety of elastic modulus ratios is considered for the analyses (Azhari and Ozbay, 2016; Gischig *et al.*, 2015; He *et al.*, 2010; Masini *et al.*, 2021; Psarropoulos *et al.*, 2007).

Psarropoulos *et al.* (2007) conducted numerical analyses investigating the effect of soil and waste characteristics on the seismic response of landfills. The numerical results proposed that in addition to the seismic excitation and the landfill geometry, material properties significantly affect the seismic response of a landfill. Gischig *et al.* (2015) conducted a distinct-element method numerical analysis on rock slope stability, evaluating the effect of geometry, stiffness contrast and compliant fractures on the wave amplification. It was concluded that the material stiffness contrast and internal fractures cause significantly larger AFs compared with the ones caused by the geometry. Azhari and Ozbay (2016) numerically examined the effect of elastic modulus contrast between the top layer and the foundation of tailings dams and natural slopes. The results showed that increasing the stiffness contrast ratio to 1:5 causes the wave acceleration to amplify up to 16

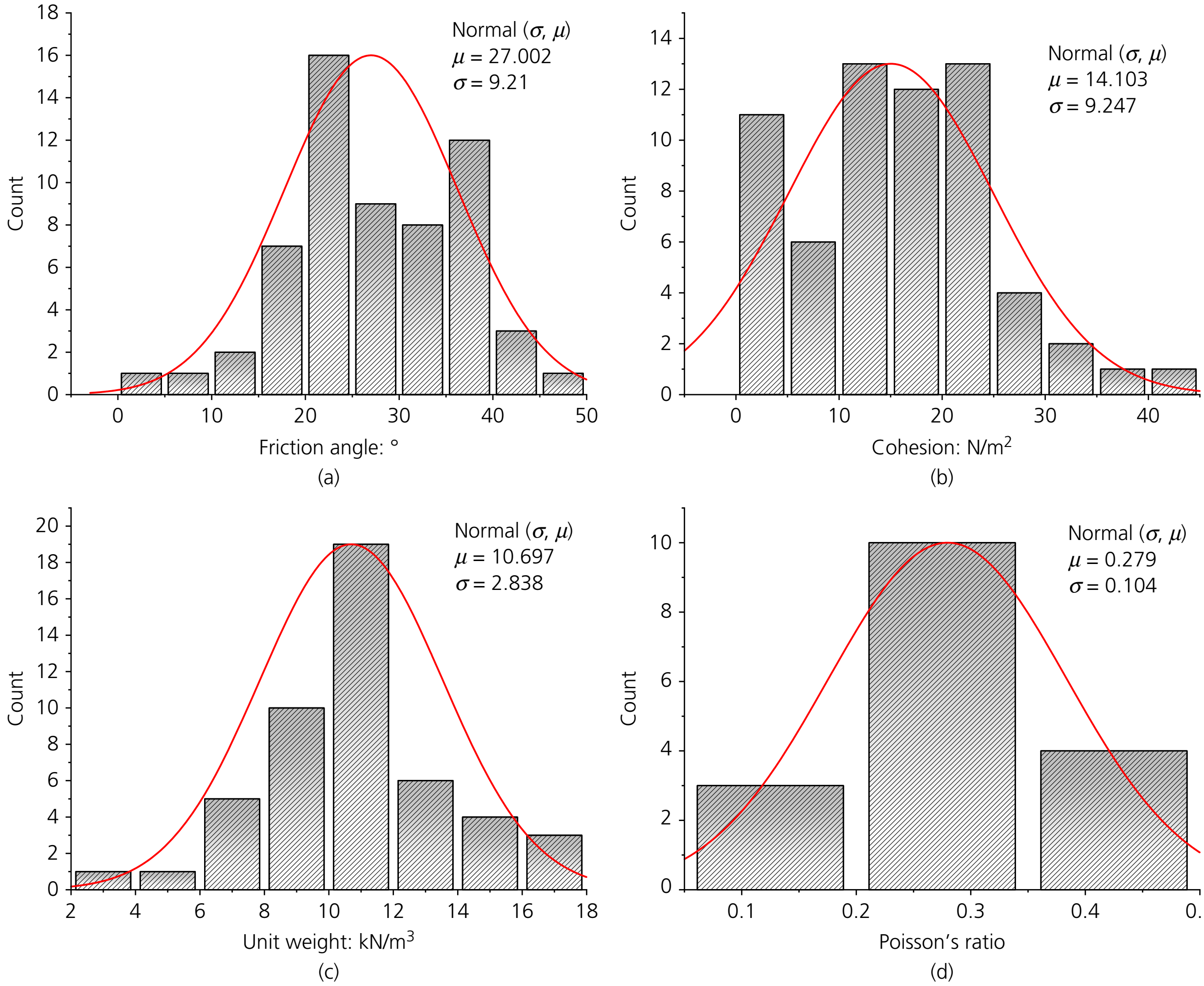

Figure 2. PDF of mechanical parameters considered in the numerical analysis: (a) PDF of friction angle, (b) PDF of cohesion, (c) PDF of unit weight, (d) PDF of Poisson's ratio

times. Masini *et al.* (2021) investigated the site conditions of earth dams in terms of stiffness contrast at the shell–core contacts resulting in various deformation patterns after an earthquake loading. He *et al.* (2010) studied the stiffness contrast of the overlying colluvium accumulation and the bedrock for a typical alluvium accumulation slope exposed to a large seismic excitation. The calculated amplifications revealed that the velocity may amplify up to 2.5 times from the bedrock to the overlying colluvium accumulation on the slope crest. According to the literature, stiffness contrast may significantly affect the seismic response of slopes, which can be observed between different layers of landfill structures, including soil base and waste material, base material and clay liner, and waste material and cover layer. In this study, the main stiffness contrast between the soil base and waste material is evaluated in four levels of 1:1, 1:2, 1:10 and 1:20, in which the elastic moduli of 5, 10, 50 and 100 MPa are selected for the simulations based on the most common municipal waste material presented in Table 3.

2.3 Dynamic analysis considerations in UDEC

Before applying the seismic load to the landfills, all models are controlled to be stable statically. Subsequently, to perform the dynamic analysis, some adjustments should apply to the static model. The first set of considerations is boundary conditions, mesh dimensions and damping ratios (Itasca Consulting Group, 2014). These requirements, if adjusted, ensure that the seismic waves travel through the medium realistically. After considering the requirements of these dynamic analyses, the next step is to apply the earthquake dynamic loading.

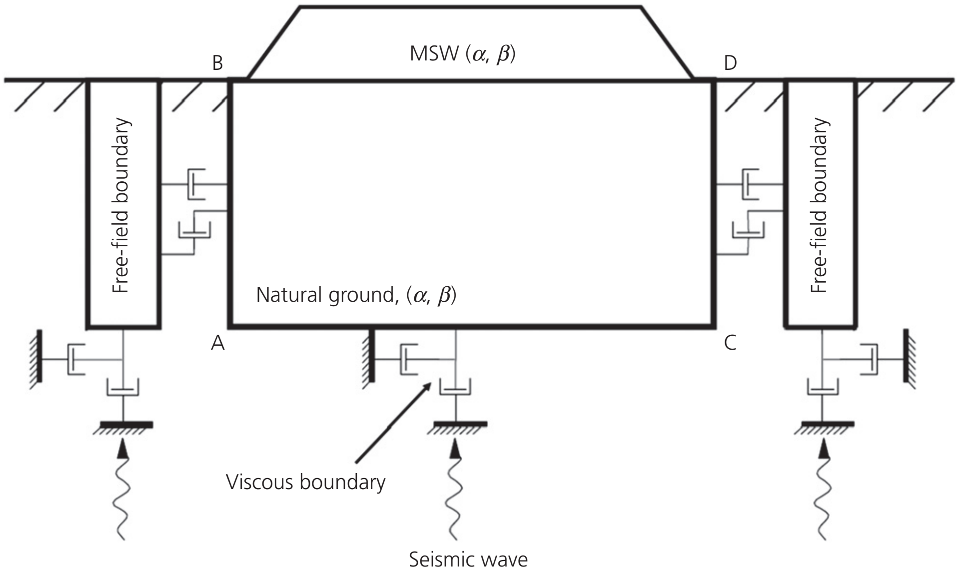

Figure 3. Boundary conditions for dynamic analysis in UDEC (source: Itasca Consulting Group (2014))

The fixed boundaries in the static analysis will reflect the seismic waves into the model. Therefore, to prevent the seismic shear wave from this phenomenon, the bottom of the model, where the seismic wave is applied, is considered viscous and the left and right model sides should be set free, so the waves are allowed to pass through these boundaries. Figure 3 depicts the boundary conditions, input wave location and damping parameters applied to the numerical model.

esh dimensions influence the wave propagation through the model, and a large mesh dimension leads to wave reflection, whereas a small mesh dimension results in considerable growth in the calculation time. The following equation determines the upper limit of mesh dimensions to ensure proper wave propagation.

1. $$l_{\max} = \frac{C_s}{10 f_{\max}} = 2.92\,\mathrm{m}$$

where C_s is the shear wave velocity and $f_{\max}$ is the maximum frequency of the waves carrying energy. Also, in order to determine the maximum mesh dimensions, the minimum shear velocity needs to be taken into account. Due to different elastic shear moduli (G), the mesh dimensions are defined and considered for each model separately.

Generally, natural dynamic systems damp a portion of oscillation energy passing through the system; otherwise, the system would vibrate constantly when subjected to a dynamic force. To mimic this phenomenon, an artificial damping is applied to the model. Proportional Rayleigh damping is typically used in the continuum analysis of the medium, to damp the natural vibration modes of the structure. Therefore, for dynamic finite-element analyses, a damping matrix, **C** (Equation 2), is formed with components proportional to the mass (**M**) and stiffness (**K**) matrices (Itasca Consulting Group, 2014). According to Zekkos (2005), the density and stiffness of the waste material increase with depth. Therefore, the damping ratio varies with depth, where the mean value is assumed for each level of elastic modulus and landfill geometry in this study.

2. $$C = \alpha M + \beta K$$

where α and β are the mass-proportional and stiffness-proportional damping constants, respectively, calculated from Equation (3), ω is the natural frequency and ξ is the damping ratio. The results of the analyses conducted by Elgamal *et al.* (2004) suggested an average constant damping of about 5.4% for MSW, utilised for the current study, and the natural frequency for the MSW models are numerically analysed as 5 Hz.

3. $$\xi = \frac{\alpha}{2\omega} + \frac{\beta\omega}{2}$$

2.3.1 Seismic wave input

The seismic load is generalised and simplified as a sinusoidal waveform, to make the results comparable for different geometries of landfill types and material properties derived from the numerical analyses. The seismic load for this study is a sinusoidal wave with a typical PGA of 1.0***g*** and a frequency of 5 Hz with a 1 s duration that lies in the common range of earthquakes. Figure 4 illustrates the harmonic wave with a duration of 1 s applied at the bottom of the model. This wave is chosen based on typical strong earthquake acceleration time histories (e.g. Northridge 1994; Canterbury 2010; Christchurch 2011 and Miyagi 2011). As noted, the AF is a parameter used to examine the seismic response of landfills during the seismic load; it is defined as the ratio of the applied earthquake acceleration to the acceleration recorded on the landfill surface. For this, the wave is applied to the bottom of the model, and the acceleration on the top of the model is monitored for calculating the AF (Mitani *et al.*, 2013; Ruan *et al.*, 2013; Tavakoli *et al.*, 2019; Wu *et al.*, 2020). According to the literature in most cases, the vertical component of the seismic wave is one-third to two-thirds of the horizontal acceleration and has a negligible effect on slope stability compared with the horizontal components that generate significant shear velocity on the slope surface (Dobry *et al.*, 2000; Frankel, 2000). Therefore, to evaluate the effect of surface acceleration better, the interaction of the surface waves from the horizontal and vertical components of the input is overlooked by only applying the horizontal wave component to the models.

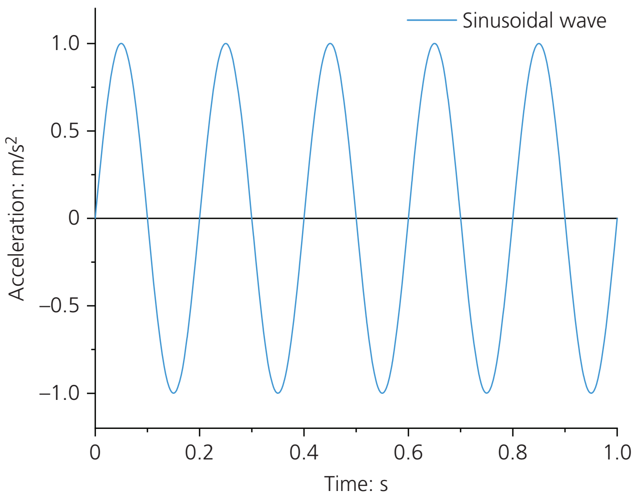

Figure 4. Sinusoidal earthquake wave applied to the model

The procedure for generating the models includes defining the geometry, boundary conditions, discretising and mesh generation, defining monitoring locations on the model bottom and slope crest and applying the seismic wave. The developed models in UDEC are shown in Figure 5. This figure illustrates the model dimensions, mesh lengths, boundary conditions and monitored locations for acceleration time histories.

3. Results and discussion

To define the AF obtained from the numerical analyses, the acceleration on the crest of each landfill type is monitored, as

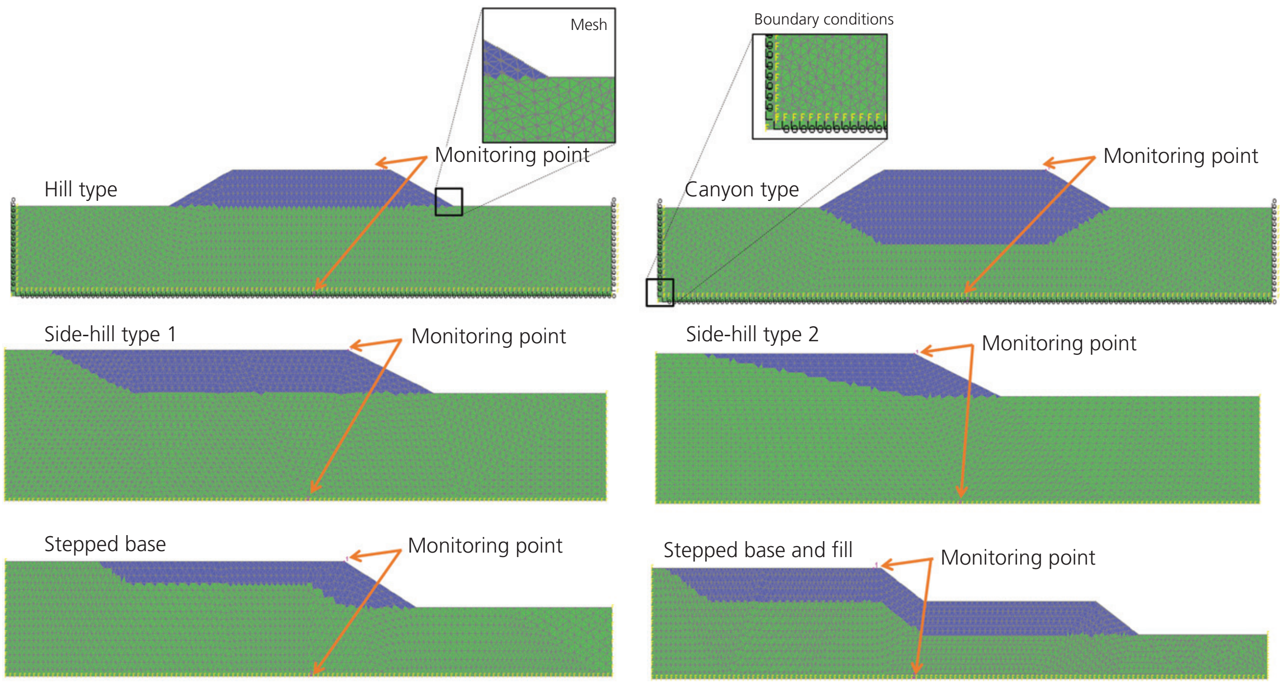

Figure 5. Generated models for six landfill types

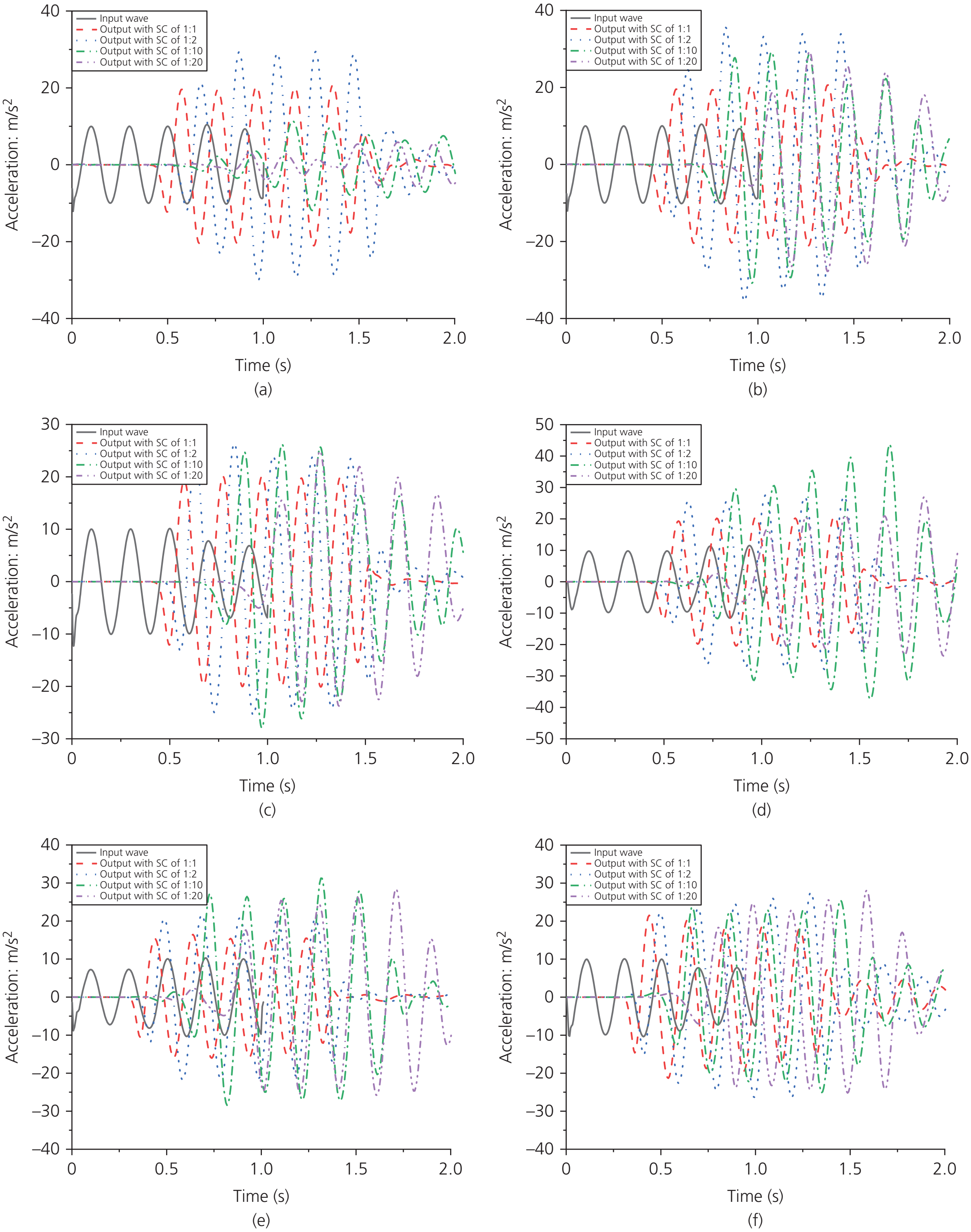

Figure 6. Recorded wave from considered landfills in four levels of stiffness contrast (SC): (a) recorded wave from canyon type, (b) recorded wave from hill type, (c) recorded wave from side-hill type 1, (d) recorded wave from side-hill type 2, (e) recorded wave from stepped-base type, (f) recorded wave from stepped-base and fill type

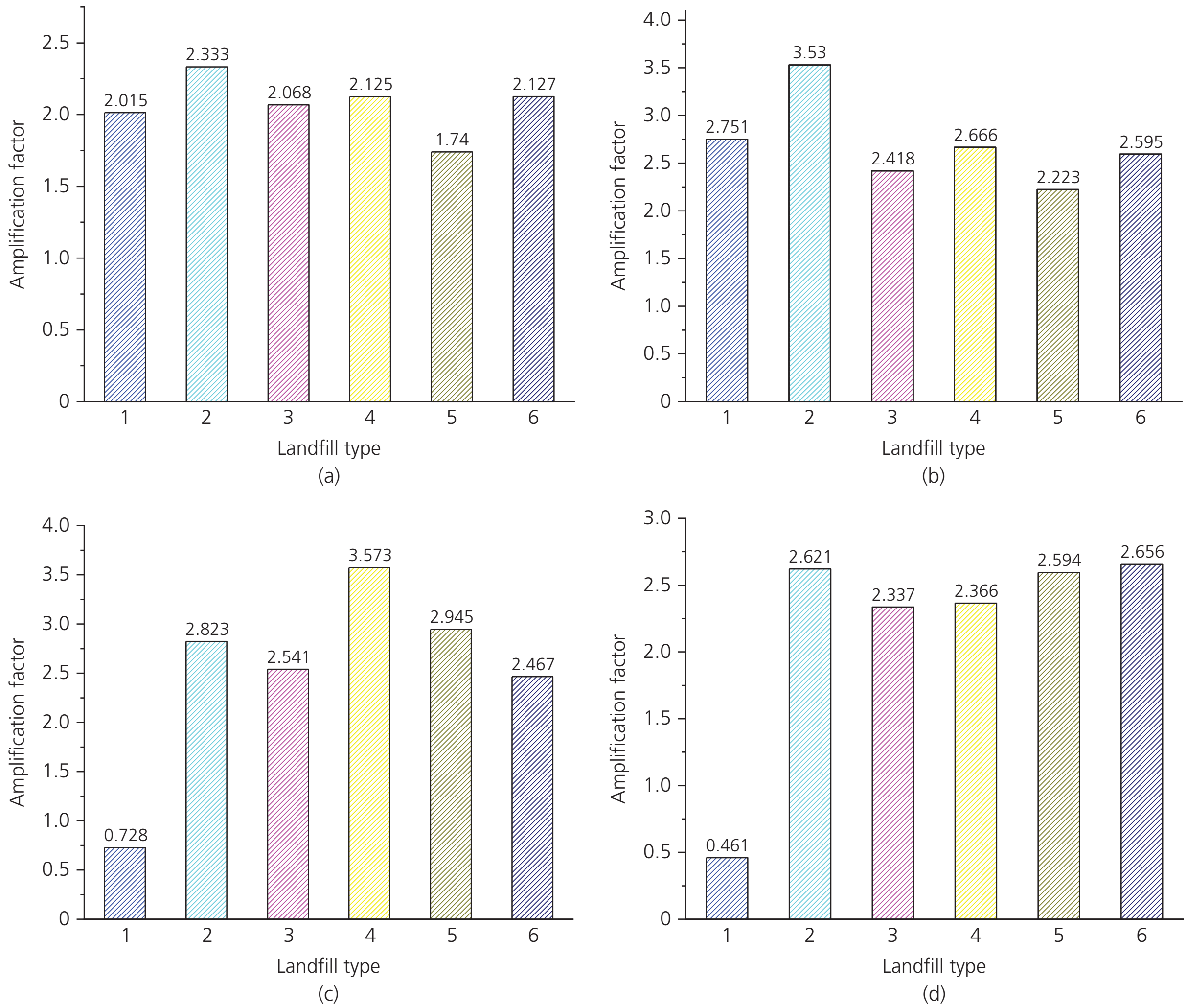

Figure 7. Effect of the geometry of six considered landfills in four levels of stiffness contrast: (a) geometry effect for each type of landfills in stiffness contrast of 1:1, (b) geometry effect of landfills in stiffness contrast of 1:2, (c) geometry effect of landfills in stiffness contrast of 1:10, (d) geometry effect of landfills in stiffness contrast of 1:20; (1) canyon type, (2) hill type, (3) side-hill type 1, (4) side-hill type 2, (5) stepped base, (6) stepped base and fill

shown in Figure 5. The obtained accelerations are then divided by the input acceleration applied to the bottom of the models to calculate the AF for each landfill type. These points are selected because they are expected to have the critical AF, as discussed in earlier studies (Bourdeau and Havenith, 2008; Del Gaudio and Wasowski, 2011; Havenith *et al.*, 2002; Moore *et al.*, 2011; Sepúlveda *et al.*, 2005; Seyhan and Stewart, 2014). Figure 6 presents the accelerations recorded on the slope crest for each group of landfills in four different stiffness levels along with the input wave acceleration.

Before discussing the results obtained, it is expected that the lower stiffness of the waste material will lead to higher AFs. However, this lower stiffness results in an increment of

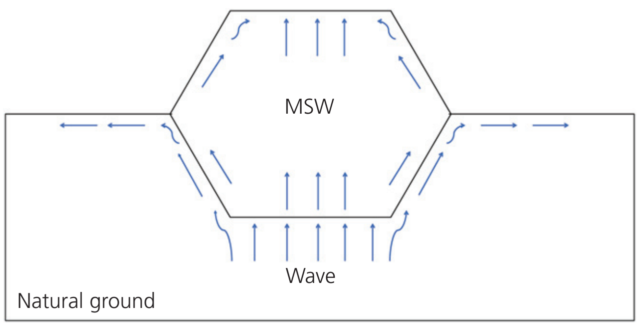

Figure 8. Wave propagation travelling through high-to-low stiffness in canyon-type geometries

damping. Moreover, the impact of the slope geometry on the wave propagation affects the topographical AF. Therefore, the interaction of the three parameters – stiffness, damping and slope geometry – affects the resulting AF.

Figure 6 shows a general increase in the wave amplitude in higher stiffness when there is a soft waste material on the top of the slope. However, a closer look at the graphs shows a non-constant trend in the wave amplitudes with stiffness contrast growth.

As shown in Figure 1, landfill types can be categorised two by two in three styles: two-sided slope, side-hill and stepped types. This section compares the earthquake response of each style group. Figure 7 illustrates the effect of geometry for each landfill type at four stiffness contrasts of 1:1, 1:2, 1:10 and 1:20. In general, a wave travelling from high-stiffness to low-stiffness material causes amplification of acceleration, where in the cases of a deep low-stiffness waste layer, the acceleration attenuates, resulting in a lower rate of AF growth. Considering low stiffness contrasts of 1:1 and 1:2, the stepped-base landfill type has the minimum and the hill type experiences the maximum AF due to their smallest and largest waste layer thickness, respectively. The other reason is the two-sided slope geometry of the canyon and hill types, causing a degree of freedom during earthquake load. On the contrary, generally in high stiffness contrasts of 1:10 and 1:20, the effect of damping leads to low AFs. As can be seen, there is a

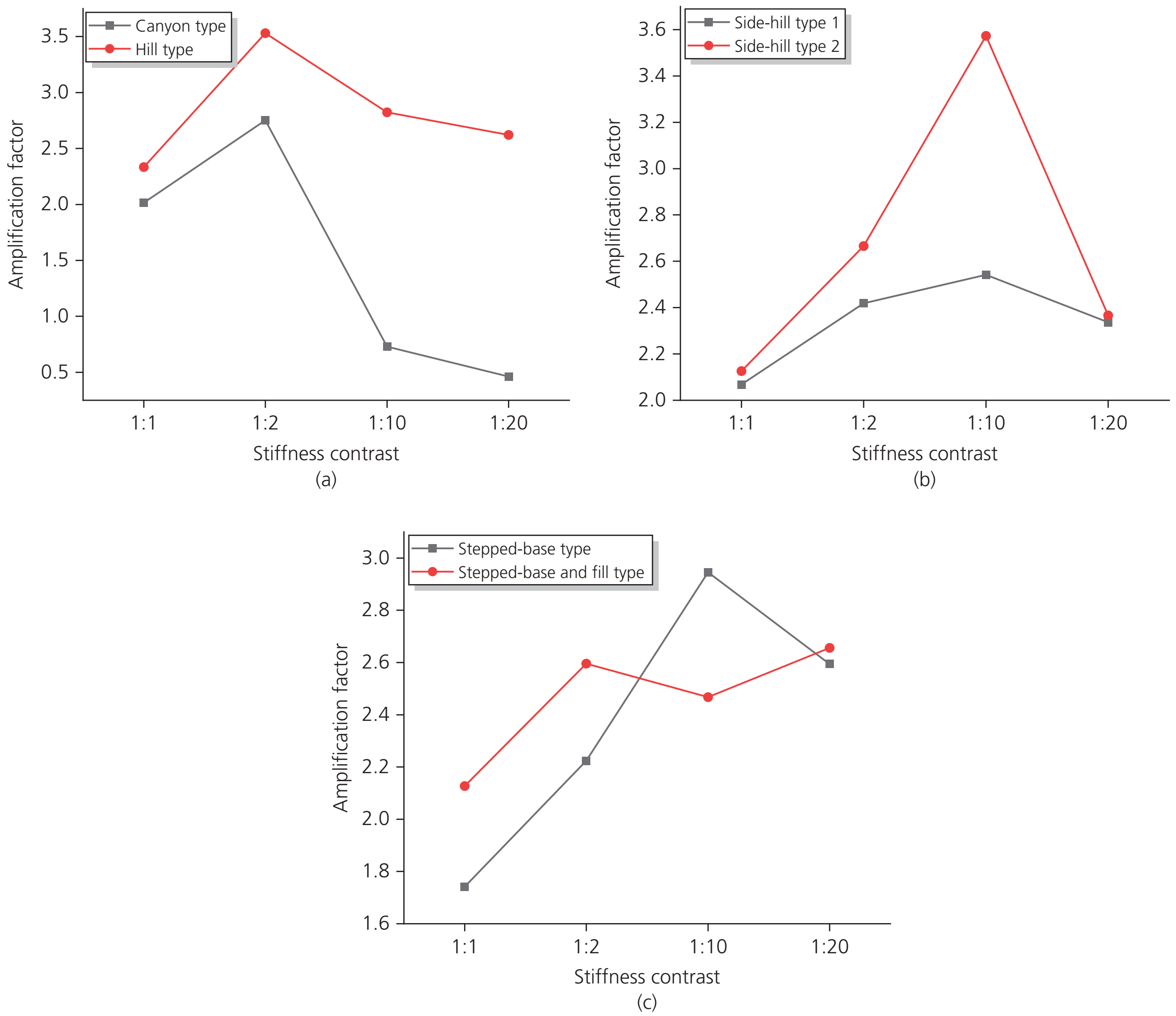

Figure 9. Amplification factor (AF) plotted against stiffness contrast for three typical landfill types: (a) AF of two-sided landfill slope, (b) AF of one-sided landfill slope, (c) AF of stepped landfill slope

significant reduction in the AF for the canyon type with high stiffness contrasts, which is a result of the superposing effect of damping, waste depth and the wave scattering phenomenon. Figure 8 illustrates the wave propagation travelling through high-to-low stiffness in canyon-type geometries.

Figure 9 depicts the AF trend in the considered stiffness contrasts for the three landfill groups. As seen in this figure, for the two-sided types (Figure 9(a)), the hill geometry experiences a larger AF, due to the thin waste layer; on increasing the stiffness contrast, the AF decreases due to the larger damping amount, and this reduction is significantly larger in the canyon type due to the deeper waste layer. Although there is a similar trend for both of these types, the canyon type shows a significantly low AF in larger stiffness contrast. As mentioned earlier, this phenomenon is expected to be observed mostly in valleys due to wave diffraction. As shown in Figure 8, the canyon-type landfill with a low material stiffness behaves similar to valleys. According to Figure 9(b), the lower thickness of waste in side-hill type 2 causes a sharper increment in AF compared with the side-hill type 1, whereas for stiffness contrasts larger than 1:10, the damping effect overcomes the wave amplification and dramatically decreases the AF for both side-hill types. Figure 9(c) depicts a general growth in the AF for stepped-base types and despite the side-hill geometries, no reduction is observed in high stiffness contrasts. This is explained by the relatively shallow waste layer compared with other geometries.

4. Conclusion

Numerical analyses are performed to evaluate the effect of stiffness contrast and geometry of six typical MSW landfill types under seismic loading. In general, the results show that the acceleration may amplify up to 3.6 in hill-type landfills with low-stiffness waste material. However, landfill types have significantly different behaviours due to their geometry and waste material properties, which is due to different interactions of the damping and wave propagation in various landfill types. The topographical site effect results in an AF of 1.7–2.3 in landfills. However, for the hill and canyon types, the maximum amplification is reached at a stiffness contrast of 1:2, and for side-hill and stepped-base types at a stiffness contrast of 1:10. Therefore, the geometry and the disposed waste material for the landfills should be considered in seismically active areas in order to control the amplification phenomenon.

It is suggested to study the effect of earthquake frequency and its ratio with the landfill height on their seismic response in future studies. Also, the seismic response can be evaluated by applying large historical earthquakes, such as El Centro, 1940, Northridge, 1994 and ChiChi, 1999, or harmonic waves such as Ricker with various amplitudes and frequencies.

REFERENCES

Abreu AES and Vilar OM (2017) Influence of composition and degradation on the shear strength of municipal solid waste. *Waste Management* **68**: 263–274, https://doi.org/10.1016/j.wasman.2017.05.038.

Azhari A and Ozbay U (2016) Evaluating the effect of earthquakes on open pit mine slopes. *50th US Rock Mechanics/Geomechanics Symposium, Houston, TX, USA*, vol. 3, pp. 2539–2547.

Azhari A and Ozbay U (2017) Investigating the effect of earthquakes on open pit mine slopes. *International Journal of Rock Mechanics and Mining Sciences* **100**: 218–228.

Azhari A and Ozbay U (2018) Role of geometry and stiffness contrast on stability of open pit mines struck by earthquakes. *Geotechnical and Geological Engineering* **36(2)**: 1249–1266, https://doi.org/10.1007/s10706-017-0390-x.

Bareither CA, Benson CH, Barlaz MA, Edil TB and Tolaymat TM (2010) Performance of North American bioreactor landfills. I: leachate hydrology and waste settlement. *Journal of Environmental Engineering* **136(8)**: 824–838.

Bourdeau C and Havenith HB (2008) Site effects modelling applied to the slope affected by the Suusamyr earthquake (Kyrgyzstan, 1992). *Engineering Geology* **97(3–4)**: 126–145, https://doi.org/10.1016/j.enggeo.2007.12.009.

Bray JD and Rathje EM (1998) Earthquake-induced displacements of solid-waste landfills. *Journal of Geotechnical and Geoenvironmental Engineering* **124(3)**: 242–253, https://doi.org/10.1061/(ASCE)1090-0241(1998)124:3(242).

Bray JD, Augello AJ, Leonards GA, Repetto PC and Byrne RJ (1995) Seismic stability procedures for solid-waste landfills. *Journal of Geotechnical Engineering* **121(2)**: 139–151, https://doi.org/10.1061/(ASCE)0733-9410(1995)121:2(139).

Caicedo B, Yamin L, Giraldo E, Coronado O and Soler N (2002) Geomechanical properties of municipal solid waste in Dona Juana sanitary landfill. In *Environmental Geotechnics: Proceedings of the Fourth International Congress on Environmental Geotechnics (4th ICEG)* (de Mello LG and Almeida M (eds)). Balkema, Rotterdam, the Netherlands, vol. 1, pp. 177–182.

Chen Y, Gao D, Zhu B and Chen R (2008) Seismic stability and permanent displacement of landfill along liners. *Science in China Series E: Technological Sciences* **51(4)**: 407–423, https://doi.org/10.1007/s11431-008-0031-y.

Choudhury D and Savoikar P (2009) Simplified method to characterize municipal solid waste properties under seismic conditions. *Waste Management* **29(2)**: 924–933, https://doi.org/10.1016/j.wasman.2008.05.008.

Choudhury D and Savoikar P (2011a) Seismic yield accelerations of MSW landfills by pseudo-dynamic approach. *Natural Hazards* **56(1)**: 275–297, https://doi.org/10.1007/s11069-010-9568-8.

Choudhury D and Savoikar P (2011b) Seismic stability analysis of expanded MSW landfills using pseudo-static limit equilibrium method. *Waste Management & Research: the Journal for a Sustainable Circular Economy* **29(2)**: 135–145, https://doi.org/10.1177/0734242X10375333.

Chugh AK, Stark TD and DeJong KA (2007) Reanalysis of a municipal landfill slope failure near Cincinnati, Ohio, USA. *Canadian Geotechnical Journal* **44(1)**: 33–53, https://doi.org/10.1139/t06-089.

Cowland JW, Tang KY and Gabay J (1993) Density and strength properties of Hong Kong refuse. *Fourth International Landfill Symposium, Sardinia, Italy*, pp. 1433–1446.

Del Gaudio V and Wasowski J (2011) Advances and problems in understanding the seismic response of potentially unstable slopes.

Engineering Geology **122(1–2)**: 73–83, https://doi.org/10.1016/j.enggeo.2010.09.007.

Del Greco O and Oggeri C (1994) Shear resistance tests on municipal solid wastes. *First International Conference on Environmental Geotechnics, Edmonton, AL, Canada.*

Dixon N and Jones DRV (2005) Engineering properties of municipal solid waste. *Geotextiles and Geomembranes* **23(3)**: 205–233, https://doi.org/10.1016/j.geotexmem.2004.11.002.

Dixon N, Jones DRV and Fowmes GJ (2006) Interface shear strength variability and its use in reliability-based landfill stability analysis. *Geosynthetics International* **13(1)**: 1–14, https://doi.org/10.1680/gein.2006.13.1.1.

Dobry R, Borcherdt RD, Crouse CB *et al.* (2000) New site coefficients and site classification system used in recent building seismic code provisions. *Earthquake Spectra* **16(1)**: 41–67, https://doi.org/10.1193/1.1586082.

Elgamal A, Lai T, Gunturi R and Zeghal M (2004) System identification of landfill seismic response. *Journal of Earthquake Engineering* **8(4)**: 545–566.

Fakharian K and Taherzadeh R (2004) Seismic response and stability analysis of an area method MSW landfill. *Proceedings of the 13th World Conference on Earthquake Engineering, Vancouver, Canada*, p. 3143.

Fassett JB, Leonards GA and Repetto PC (1994) Geotechnical properties of municipal solid wastes and their use in landfill design. *Waste Tech '94, Silver Springs, MD, USA.*

Fatahi B and Khabbaz H (2013) Influence of fly ash and quicklime addition on behaviour of municipal solid wastes. *Journal of Soils and Sediments* **13(7)**: 1201–1212, https://doi.org/10.1007/s11368-013-0720-4.

Feng SJ (2005) *Static and Dynamic Strength Properties of Municipal Solid Waste and Stability Analyses of Landfill*. Zhejiang University, Hangzhou, China (in Chinese).

Feng SJ, Gao KW, Chen YX *et al.* (2017) Geotechnical properties of municipal solid waste at Laogang landfill, China. *Waste Management* **63**: 354–365, https://doi.org/10.1016/j.wasman.2016.09.016.

Feng SJ, Chang JY and Chen HX (2018) Seismic analysis of landfill considering the effect of GM-GCL interface within liner. *Soil Dynamics and Earthquake Engineering* **107**: 152–163, https://doi.org/10.1016/j.soildyn.2018.01.025.

Frankel A (2000) Three-dimensional simulations of ground motions in the Seattle Region for earthquakes in the Seattle fault zone. *Bulletin of the Seismological Society of America* **90(5)**: 1251–1267, https://doi.org/10.1785/0119990159.

Gabr MA and Valero SN (1995) Geotechnical properties of municipal solid waste. *Geotechnical Testing Journal* **18(2)**: 241–251, https://doi.org/10.1520/GTJ10324J.

Giri RK and Reddy KR (2014) Design charts for selecting minimum setback distance from side slope to horizontal trench system in bioreactor landfills. *Geotechnical and Geological Engineering* **32(4)**: 1017–1027, https://doi.org/10.1007/s10706-014-9777-0.

Giri RK and Reddy KR (2015) Slope stability of bioreactor landfills during leachate injection: effects of geometric configurations of horizontal trench systems. *Geomechanics and Geoengineering* **10(2)**: 126–138, https://doi.org/10.1080/17486025.2014.921335.

Gischig VS, Eberhardt E, Moore JR and Hungr O (2015) On the seismic response of deep-seated rock slope instabilities – insights from numerical modeling. *Engineering Geology* **193**: 1–18, https://doi.org/10.1016/j.enggeo.2015.04.003.

Grisolia M, Napoleoni Q and Tancredi G (1995) The use of triaxial tests for the mechanical characterization of municipal solid waste. *Proceedings of the 5th International Landfill Symposium, Sardinia, Italy*, vol. 2, pp. 761–767.

Harris JM, Shafer AL, DeGroff W *et al.* (2005) Shear strength of degraded reconsitituted municipal solid waste. *Geotechnical Testing Journal* **29(2)**: 141–148, https://doi.org/10.1520/GTJ14089.

Havenith HB, Jongmans D, Faccioli E, Abdrakhmatov K and Bard PY (2002) Site effect analysis around the seismically induced Ananevo rockslide, Kyrgyzstan. *Bulletin of the Seismological Society of America* **92(8)**: 3190–3209, https://doi.org/10.1785/0120010206.

Havenith HB, Vanini M, Jongmans D and Faccioli E (2003) Initiation of earthquake-induced slope failure: influence of topographical and other site specific amplification effects. *Journal of Seismology* **7(3)**: 397–412, https://doi.org/10.1023/A:1024534105559.

He J, Li X, Li S, Yin Y and Qian H (2010) Study of seismic response of colluvium accumulation slope by particle flow code. *Granular Matter* **12(5)**: 483–490, https://doi.org/10.1007/s10035-010-0213-8.

Hossain MS, Santhanam A, Nik Norulaini NA and Omar AKM (2011) Clinical solid waste management practices and its impact on human health and environment – a review. *Waste Management* **31(4)**: 754–766, https://doi.org/10.1016/j.wasman.2010.11.008.

Houston WN, Houston SL, Liu JW, Elsayed A and Sanders CO (1995) In-situ testing methods for dynamic properties of MSW landfills. In *Earthquake Design and Performance of Solid Waste Landfills* (Yegian MK and Finn WDL (eds)). American Society of Civil Engineers, New York, NY, USA, Geotechnical Special Publication no. 54, pp. 73–82.

Hubert J, Liu XF and Collin F (2016) Numerical modeling of the long term behavior of municipal solid waste in a bioreactor landfill. *Computers and Geotechnics* **72**: 152–170, https://doi.org/10.1016/j.compgeo.2015.10.007.

IBRD (The International Bank for Reconstruction and Development) (2019) *Trends in Solid Waste Management*. The World Bank, Washington, DC, USA. See https://datatopics.worldbank.org/what-a-waste/trends_in_solid_waste_management.html (accessed 16/07/2021).

Isfahani HS, Abtahi SM, Roshanzamir MA, Shirani A and Hejazi SM (2019) Investigation on gamma-ray shielding and permeability of clay-steel slag mixture. *Bulletin of Engineering Geology and the Environment* **78(6)**: 4589–4598, https://doi.org/10.1007/s10064-018-1391-6.

Itasca Consulting Group (2014) *UDEC (Universal Distinct Element Code), Version 6.0. User Manual*. Itasca Consulting Group, Minneapolis, MN, USA.

Jahanfar MA (2014) *Landfill Slope Stability Risk Assessment*. Master's thesis, University of Guelph, Guelph, ON, Canada.

Jones DRV and Dixon N (2005) Landfill lining stability and integrity: the role of waste settlement. *Geotextiles and Geomembranes* **23(1)**: 27–53, https://doi.org/10.1016/j.geotexmem.2004.08.001.

Kavazanjian E, Matasovic N, Bonaparte R and Schmertmann GR (1995) Evaluation of MSW properties for seismic analysis. In *Geoenvironment 2000: Characterization, Containment, Remediation, and Performance in Environmental Geotechnics* (Acar YB and Daniel DE (eds)). American Society of Civil Engineers, New York, NY, USA, Geotechnical Special Publication no. 46, vol. 2, pp. 1126–1141.

Koelsch F, Fricke K, Mahler C and Damanhuri E (2005) Stability of landfills – the Bandung dumpsite disaster. In *Sardinia 2005: 10th International Waste Management and Landfill Symposium Proceedings* (Cossu R and Stegmann R (eds)). CISA Publisher, Padova, Italy (CD-ROM).

Kramer SL and Smith MW (1997) Modified Newmark model for seismic displacements of compliant slopes. *Journal of Geotechnical and*

Geoenvironmental Engineering **123(7)**: 635–644, https://doi.org/10.1061/(ASCE)1090-0241(1997)123:7(635).

Landva AO and Clark JI (1990) Geotechnics of waste fill. In *Geotechnics of Waste Fills – Theory and Practice* (Landva A and Knowles GD (eds)). ASTM International, West Conshohocken, PA, USA, Special Technical Publication no. 1070, pp. 86–103.

Landva A and Knowles GD (eds) (1990) *Geotechnics of Waste Fills – Theory and Practice*. ASTM International, West Conshohocken, PA, USA, Special Technical Publication no. 1070.

Ling HI and Leshchinsky D (1997) Seismic stability and permanent displacement of landfill cover systems. *Journal of Geotechnical and Geoenvironmental Engineering* **123(2)**: 113–122, https://doi.org/10.1061/(ASCE)1090-0241(1997)123:2(113).

Ling H, Ling HI and Kawabata T (2015) Revisiting Nigawa landslide of the 1995 Kobe earthquake. *Géotechnique* **64(5)**: 149–153, https://doi.org/10.1680/geot.12.T.019.

Machado SL, Carvalho MF and Vilar OM (2002) Constitutive model for municipal solid waste. *Journal of Geotechnical and Geoenvironmental Engineering* **128(11)**: 940–951, https://doi.org/10.1061/(ASCE)1090-0241(2002)128:11(940).

Masini L, Rampello S and Donatelli R (2021) Seismic performance of two classes of earth dams. *Earthquake Engineering & Structural Dynamics* **50(2)**: 692–711, https://doi.org/10.1002/eqe.3352.

Matasović N and Kavazanjian E (1998) Cyclic characterization of OII landfill solid waste. *Journal of Geotechnical and Geoenvironmental Engineering* **124(3)**: 197–210, https://doi.org/10.1061/(ASCE)1090-0241(1998)124:3(197).

Matasovic N, El-Sherbiny R and Kavazanjian E Jr (2011) In-situ measurements of MSW properties. In *Geotechnical Characterization, Field Measurement, and Laboratory Testing of Municipal Solid Waste* (Zekkos D (ed.)). American Society of Civil Engineers, Reston, VA, USA, pp. 153–194.

Merry SM, Kavazanjian E and Fritz WU (2005) Reconnaissance of the July 10, 2000, Payatas landfill failure. *Journal of Performance of Constructed Facilities* **19(2)**: 100–107, https://doi.org/10.1061/(ASCE)0887-3828(2005)19:2(100).

Meunier P, Hovius N and Haines JA (2008) Topographic site effects and the location of earthquake induced landslides. *Earth and Planetary Science Letters* **275(3–4)**: 221–232, https://doi.org/10.1016/j.epsl.2008.07.020.

Misra V and Pandey SD (2005) Hazardous waste, impact on health and environment for development of better waste management strategies in future in India. *Environment International* **31(3)**: 417–431, https://doi.org/10.1016/j.envint.2004.08.005.

Mitani Y, Wang F, Okeke AC and Qi W (2013) Dynamic analysis of earthquake amplification effect of slopes in different topographic and geological conditions by using ABAQUS. In *Progress of Geo-Disaster Mitigation Technology in Asia* (Wang F, Miyajima M, Li T *et al.* (eds)). Springer, Berlin, Germany, pp. 469–490.

Modak P (2010) Municipal solid waste management: turning waste into resources. In *Shanghai Manual – a Guide for Sustainable Urban Development in the 21st Century*. UN, New York, NY, USA, ch. 5.

Moore JR, Gischig V, Burjanek J, Loew S and Fah D (2011) Site effects in unstable rock slopes: dynamic behavior of the Randa instability (Switzerland). *Bulletin of the Seismological Society of America* **101(6)**: 3110–3116, https://doi.org/10.1785/0120110127.

Ouyang C, Zhou K, Xu Q *et al.* (2017) Dynamic analysis and numerical modeling of the 2015 catastrophic landslide of the construction waste landfill at Guangming, Shenzhen, China. *Landslides* **14(2)**: 705–718, https://doi.org/10.1007/s10346-016-0764-9.

Pelkey SA, Valsangkar AJ and Landva A (2001) Shear displacement dependent strength of municipal solid waste and its major constituent. *Geotechnical Testing Journal* **24(4)**: 381–390, https://doi.org/10.1520/GTJ11135J.

Psarropoulos PN, Tsompanakis Y and Karabatsos Y (2007) Effects of local site conditions on the seismic response of municipal solid waste landfills. *Soil Dynamics and Earthquake Engineering* **27(6)**: 553–563, https://doi.org/10.1016/j.soildyn.2006.10.004.

Ramaiah BJ, Ramana GV and Datta M (2017) Mechanical characterization of municipal solid waste from two waste dumps at Delhi, India. *Waste Management* **68**: 275–291, https://doi.org/10.1016/j.wasman.2017.05.055.

Rathje EM and Bray JD (2001) One- and two-dimensional seismic analysis of solid-waste landfills. *Canadian Geotechnical Journal* **38(4)**: 850–862, https://doi.org/10.1139/cgj-38-4-850.

Reddy KR, Hettiarachchi H, Gangathulasi J and Bogner JE (2011) Geotechnical properties of municipal solid waste at different phases of biodegradation. *Waste Management* **31(11)**: 2275–2286, https://doi.org/10.1016/j.wasman.2011.06.002.

Ruan X, Sun S and Liu W (2013) Effect of the amplification factor on seismic stability of expanded municipal solid waste landfills using the pseudo-dynamic method. *Journal of Zhejiang University Science A* **14(10)**: 731–738, https://doi.org/10.1631/jzus.A1300041.

Savoikar P and Choudhury D (2010) Computation of pseudo-static yield accelerations of landfills. *International Journal of Geotechnical Engineering* **4(3)**: 305–317, https://doi.org/10.3328/IJGE.2010.04.03.305-317.

Sepúlveda SA, Murphy W, Jibson RW and Petley DN (2005) Seismically induced rock slope failures resulting from topographic amplification of strong ground motions: the case of Pacoima Canyon, California. *Engineering Geology* **80(3–4)**: 336–348, https://doi.org/10.1016/j.enggeo.2005.07.004.

Seyhan E and Stewart JP (2014) Semi-empirical nonlinear site amplification from NGA-West2 data and simulations. *Earthquake Spectra* **30(3)**: 1241–1256, https://doi.org/10.1193/063013EQS181M.

Shinoda M, Watanabe K, Kojima K, Tateyama M and Horii K (2009) Seismic stability of a reinforced-soil structure constructed after the mid-Niigata prefecture earthquake. *Geosynthetics International* **16(4)**: 274–285, https://doi.org/10.1680/gein.2009.16.4.274.

Shu S, Zhu W, Wang S *et al.* (2018) Leachate breakthrough mechanism and key pollutant indicator of municipal solid waste landfill barrier systems: centrifuge and numerical modeling approach. *Science of The Total Environment* **612**: 1123–1131, https://doi.org/10.1016/j.scitotenv.2017.08.185.

Si H and Midorikawa S (2000) New attenuation relations for peak ground acceleration and velocity considering effects of fault type and site condition. In *Proceedings of the 12th World Conference on Earthquake Engineering*. New Zealand Society for Earthquake Engineering, Upper Hutt, New Zealand, paper 0532.

Sia AHI and Dixon N (2012) Numerical modelling of landfill lining system-waste interaction: implications of parameter variability. *Geosynthetics International* **19(5)**: 393–408, https://doi.org/10.1680/gein.12.00025.

Siegel R, Robertson R and Anderson D (1990) Slope stability investigations at a landfill in Southern California. In *Geotechnics of Waste Fills – Theory and Practice* (Landva A and Knowles GD (eds)). ASTM International, West Conshohocken, PA, USA, Special Technical Publication no. 1070, pp. 259–284.

Singh MK, Sharma JS and Fleming IR (2009a) A design chart for estimation of horizontal displacement in municipal landfills. *Waste Management* **29(5)**: 1577–1587, https://doi.org/10.1016/j.wasman.2008.10.003.

Singh MK, Sharma JS and Fleming IR (2009b) Shear strength testing of intact and recompacted samples of municipal solid waste. *Canadian Geotechnical Journal* **46(10)**: 1133–1145, https://doi.org/10.1139/t09-052.

Stoltz G, Nousheen KN, Gourc JP, Olivier F and Redon E (2009) Hydro-mechanical properties of MSW from laboratory tests following a deep drilling campaign. In *Sardinia 2009: 12th International Waste Management and Landfill Symposium Proceedings* (Cossu R (ed.)). CISA Publisher, Padova, Italy (CD-ROM).

Tano BFG, Dias D, Fowmes GJ *et al.* (2016) Numerical modeling of the nonlinear mechanical behavior of multilayer geosynthetic system for piggyback landfill expansions. *Geotextiles and Geomembranes* **44(6)**: 782–798, https://doi.org/10.1016/j.geotexmem.2016.07.004.

Tano BFG, Dias D, Stoltz G, Touze-Foltz N and Olivier F (2017) Numerical modelling to identify key factors controlling interface behaviour of geosynthetic lining systems. *Geosynthetics International* **24(2)**: 167–183, https://doi.org/10.1680/jgein.16.00024.

Tavakoli H, Kutanaei SS and Hosseini SH (2019) Assessment of seismic amplification factor of excavation with support system. *Earthquake Engineering and Engineering Vibration* **18(3)**: 555–566, https://doi.org/10.1007/s11803-019-0521-x.

Varga G (2011) Some geotechnical aspects of bioreactor landfills. *Periodica Polytechnica Civil Engineering* **55(1)**: 39–44, https://doi.org/10.3311/pp.ci.2011-1.05.

Wang S and Hao H (2002) Effects of random variations of soil properties on site amplification of seismic ground motions. *Soil Dynamics and Earthquake Engineering* **22(7)**: 551–564, https://doi.org/10.1016/S0267-7261(02)00038-6.

Withiam JL, Tarvin PA, Bushell TD, Snow RE and Germann HW (1995) Prediction and performance of municipal landfill slope. In *Geoenvironment 2000: Characterization, Containment, Remediation, and Performance in Environmental Geotechnics* (Acar YB and Daniel DE (eds)). American Society of Civil Engineers, New York, NY, USA, Geotechnical Special Publication no. 46, vol. 2, pp. 1005–1019.

Wu Z, Zhang D, Wang S, Liang C and Zhao D (2020) Dynamic-response characteristics and deformation evolution of loess slopes under seismic loads. *Engineering Geology* **267**: 105507, https://doi.org/10.1016/j.enggeo.2020.105507.

Yu L and Batlle F (2011) A hybrid method for quasi-three-dimensional slope stability analysis in a municipal solid waste landfill. *Waste Management* **31(12)**: 2484–2496, https://doi.org/10.1016/j.wasman.2011.07.012.

Zamara KA, Dixon N, Fowmes G, Jones DRV and Zhang B (2014) Landfill side slope lining system performance: a comparison of field measurements and numerical modelling analyses. *Geotextiles and Geomembranes* **42(3)**: 224–235, https://doi.org/10.1016/j.geotexmem.2014.03.003.

Zania V, Tsompanakis Y and Psarropoulos PN (2008) Seismic distress and slope instability of municipal solid waste landfills. *Journal of Earthquake Engineering* **12(2)**: 312–340, https://doi.org/10.1080/13632460701574605.

Zekkos DP, Bray JD, Kavazanjian E *et al.* (2005) Framework for the estimationof MSW unit weight profile. In *Sardinia 2005: 10th International Waste Management and Landfill Symposium Proceedings* (Cossu R and Stegmann R (eds)). CISA Publisher, Padova, Italy (CD-ROM).

Zekkos D, Bray JD and Riemer MF (2008) Shear modulus and material damping of municipal solid waste based on large-scale cyclic triaxial testing. *Canadian Geotechnical Journal* **45(1)**: 45–58, https://doi.org/10.1139/t07-069.

Zhan TLT, Chen YM and Ling WA (2008) Shear strength characterization of municipal solid waste at the Suzhou landfill, China. *Engineering Geology* **97(3–4)**: 97–111, https://doi.org/10.1016/j.enggeo.2007.11.006.